Cosmic Magnetic Fields:
From Planets, to Stars and Galaxies
Proceedings IAU Symposium No. 259, 2008
K.G. Strassmeier, A.G. Kosovichev & J. Beckman, eds.

doi:10.1017/S1743921309030440

Magnetic reconnection and energy release on the Sun and solar-like stars

Lidia van Driel-Gesztelyi[1,2,3]

[1]University College London, Mullard Space Science Laboratory, Holmbury St. Mary, Dorking, Surrey, RH5 6NT, U.K.

[2]Konkoly Observatory of Hungarian Academy of Sciences, Budapest, Hungary

[3]Observatoire de Paris, LESIA, FRE 2461(CNRS), F-92195 Meudon Principal Cedex, France
email: Lidia.vanDriel@obspm.fr

Abstract. Magnetic reconnection is thought to play an important role in liberating free energy stored in stressed magnetic fields. The consequences vary from undetectable nanoflares to huge flares, which have signatures over a wide wavelength range, depending on e.g. magnetic topology, free energy content, total flux, and magnetic flux density of the structures involved. Events of small energy release, which are thought to be the most numerous, are one of the key factors in the existence of a hot corona in the Sun and solar-like stars. The majority of large flares are ejective, i.e. involve the expulsion of large quantities of mass and magnetic field from the star. Since magnetic reconnection requires small length-scales, which are well below the spatial resolution limits of even the solar observations, we cannot directly observe magnetic reconnection happening. However, there is a plethora of indirect evidences from X-rays to radio observations of magnetic reconnection. I discuss key observational signatures of flares on the Sun and solar-paradigm stellar flares and describe models emphasizing synergy between observations and theory.

Keywords. Sun: flares – Sun: magnetic fields – stars: activity – stars: flare – stars: magnetic fields

1. Introduction

Magnetic reconnection is a topological restructuring of a magnetic field, which *per definition*, leads to a change in the connectivity of its field lines. It allows the release of free magnetic energy, i.e. above the potential, zero-current, energy, which is stored in a force-free magnetic system in the form of field-aligned electric currents. During magnetic reconnection free magnetic energy is converted into kinetic energy of fast particles, mass motions and radiation across the entire electromagnetic spectrum manifested in sudden brightening i.e. a flare.

The Sun is the best-observed star in the Universe and solar physics is in a privileged position of having a fleet of spacecraft and ground-based telescopes which are able to resolve details in the solar photosphere and chromosphere as small as $0.2''$ ($\approx$140 km) and coronal structures of about $1''$ ($\approx$700 km). However, even with such fine spatial resolution nobody has been able to *directly observe* magnetic reconnection or the energy release site in the solar atmosphere. This is mainly due to the small size and low brightness of the magnetic reconnection region. There are very small length-scales needed for the breakdown of ideal magneto-hydrodynamic (MHD) conditions in a low plasma-β environment, like the solar corona, which are satisfied in thin current sheets, whose scale is orders of magnitudes lower than that of our finest spatial resolution. Furthermore, the reconnection region has low plasma density and therefore low emission measure, making its observation very difficult in the optically thin corona.

However, there is no doubt that magnetic reconnection is taking place on the Sun at all scales: There are plenty of *indirect evidences* provided by multi-wavelength observations to prove it. In this paper I select some of the highlights of solar observational signatures of magnetic reconnection and discuss observations and models of the consequent energy release events. Furthermore, I use the solar paradigm to draw parallels between solar and stellar flares and coronal heating on the Sun and stars, pointing out the differences which may originate in the differences of magnetic flux, flux density, complexity and perhaps levels of non-potentiality between the Sun and solar-like stars.

2. Solar and stellar flares - observations and models

2.1. *Classification of solar flares*

Energy released up to 10^{25} J = 10^{32} erg in the largest solar flares. Many more much smaller flare-like events occur (micro-flares, nano-flares), down to energies of 10^{24} erg and even less. GOES (Geostationary Environmental Operational Satellites) soft X-ray (SXR) classification is most common these days due to the readily available, long and continuous dataset of solar X-ray emission. The flux in the 1- 8 Å = 0.1-0.8 nm range is classified with the letters of X, M, C, B indicating flux of $10^{-4}, 10^{-5}, 10^{-6}, 10^{-7}$ W m^2, respectively. According to this classification an X2 flare has a flux of 2×10^6 Wm^{-2}.

2.2. *Origin and storage of free magnetic energy*

There is plenty of observational evidence indicating that magnetic flux emerges twisted i.e. in a non-potential state from the solar interior, carrying free energy which is ready to be released (Leka *et al.* 1996; for a recent review see Démoulin 2007a). MHD simulations have shown that untwisted flux cannot even make it through the convection zone because it gets eroded by vortexes forming in its wake (Schüssler 1979; Longcope *et al.* 1996), however, sufficient twist can prevent significant fragmentation (Moreno-Insertis & Emonet 1996). These simulation results imply that all the large-scale flux that has crossed the convection zone must be twisted.

However, the observed twist is not strong, as it was deduced from photospheric current helicity measurements (Longcope *et al.* 1999). The coronal helicity content of ARs also appears to be modest being equivalent to that of a twisted flux tube having 0.2 turn ($\mathbf{H}_{max}(\mathrm{AR}) \approx 0.2\Phi^2$, where Φ is the total magnetic flux of the AR; Démoulin 2007a). More recent simulations by Fan (2008) also suggest that in order to comply with Joy's law (a systematic deviation from the east-west alignment of bipolar ARs with the leading spots being closer to the equator on both solar hemispheres which results from the action of Coriolis force) the twist-induced tilt in rising flux ropes, which is in the opposite sense than that of the Coroilis force, cannot be as high as expected. In order for the emerging tube to show the tilt direction consistent with observations, the initial twist rate of the flux tube needs to be less than half of that needed for a cohesive rise. Under such conditions, severe flux loss was found during the rise, with less than 50% of the initial flux remaining in the Ω-tube by the time it reaches the surface.

Before the discovery that flux is emerging twisted from the solar interior, the generally accepted idea was that free magnetic energy in an active region is generated by shearing flows, which move opposite polarity footpoints in anti-parallel directions on both sides of a magnetic neutral line. There are indeed large-scale flows in the solar photosphere (e.g. differential rotation) and local deviations are clearly seen from the mean differential rotation rate in flow-maps of the solar surface (e.g. Sobotka 1999 and Meunier 2005) as well as in the solar interior, especially around active regions (Zhao & Kosovichev 2004; Švanda *et al.* 2008). Surface shearing flows can result from the emergence of a flux

https://doi.org/10.1017/S1743921309030440 Published online by Cambridge University Press

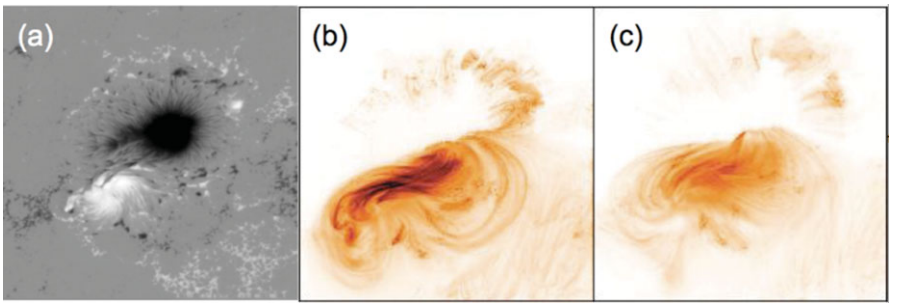

Figure 1. (*a*) *Hinode*/SOT magnetogram of AR 10930 on 13 December 2006. Integrated electric currents in the AR (*b*) before and (*c*) after an X3.4 flare. Note the current filaments' organization into an apparent flux-rope structure along the IL (adapted from Schrijver *et al.* 2008).

rope (Démoulin & Berger 2003) due to the Lorenz force arising from the nonuniform expansion of the magnetic field in a highly pressure-stratified atmosphere (Manchester 2007). Flux rope emergence has many caveats, *e.g.* in the concave-up parts under the flux rope axis plasma accumulates, leading to a fragmentation of the emerging flux rope (e.g., Magara 2004; Manchester *et al.* 2004) which can only emerge through many small-scale reconnections (Pariat *et al.* 2004). Nevertheless, characteristic magnetic patterns in emerging flux regions originating from the changing azimuthal component of a flux rope while crossing the photosphere, the so-called "magnetic tongues" (López-Fuentes *et al.* 2000; Démoulin & Pariat 2008) indicate that there is an overall organization in the emerging flux tube, which is compatible with a global twist. Besides organised motion patterns random magnetic footpoint motions (shuffling) are considered important to entangle field lines leading to the formation of small-scale current sheets.

Magnetic free energy is stored relatively low in an AR $\leqslant 20$ Mm above the photosphere and may mainly be concentrated along the magnetic inversion line in the filament channel in form of current filaments (Figure 1; Schrijver *et al.* 2008). This is supported by a strong connection found between high-gradient, strong-field magnetic inversion lines and flaring in active regions by Schrijver (2007), who introduced a new metric, R, the summed unsigned magnetic flux of the overlap of positive and negative magnetic field areas, where $B \leqslant 150$ Mx cm^{-2} with kernels of $6'' \times 6''$. R characterises newly emerged highly non-potential magnetic fields, and appears successful in forecasting major flares. If $R \geqslant 2 \times 10^{21}$ Mx ($logR \geqslant 4.8$), the probability of M or X-flare occurrence was found to be ≈ 1, while it was almost zero if $R \leqslant \times 10^{19}$ Mx ($logR \leqslant 2.8$).

2.3. *Confined flares - quadrupolar reconnection*

Reconnection takes place (i) at nullpoints (X-points) (ii) at separatrices and their intersection, the separator and (iii) at quasi-separatrix layers (QSLs, which are the non-zero-thickness generalisations of separatrixes) even in the absence of nullpoints. As a result, four flare kernels or ribbons appear at the footpoints of reconnected loops or in the vicinity of drastic field line connectivity changes, respectively. For detailed treatment of reconnection topologies see the book by Priest & Forbes (2000) and for a recent review see Démoulin (2007b).

Along QSLs field line mapping is continuous but steep gradients are present (Démoulin *et al.* 1996). Reconnection along QSLs also occurs in a continuous manner. Field lines may slip across each other, as shown in MHD simulations (Aulanier *et al.* 2006). A recent observational confirmation in Hinode/XRT data of slip-running reconnection was shown by Aulanier *et al.* (2007).

https://doi.org/10.1017/S1743921309030440 Published online by Cambridge University Press

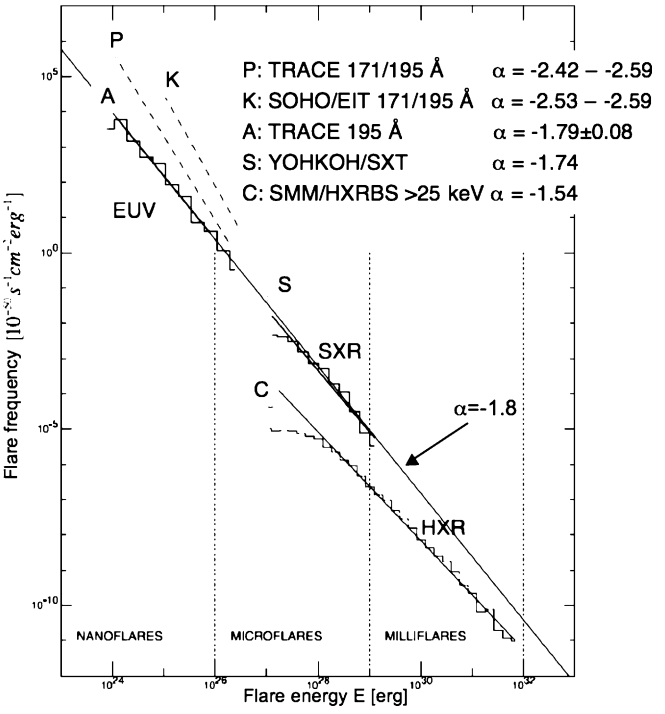

Figure 2. Powerlaws of solar flare number *versus* energy distribution adapted from Aschwanden *et al.* (2000).

2.4. *Flare frequency spectrum*

It feels natural that there are more smaller flare events than large ones. Quantifying this expectation showed that the number of flares N falls off with increasing energy E as a flat power law with a slope of $\alpha \approx -1.8$ (HXR, SXR, EUV, microwave bursts, optical flares; see Hudson 1991 and references therein). $dN/dE = A \times E^{\alpha}$ (erg s)$^{-1}$, where A normalisation factor varies with the level of activity. For the Sun, α values were found to be between -1.5 and -2.6 (Figure 2; Aschwanden *et al.* 2000 and references therein). Large flares do not supply sufficient energy to heat the solar corona (Hudson 1991). The significance of the α value is that if $\alpha \geqslant 2$, then smaller flares contribute enough to provide heating for the corona equal to its radiative losses.

Parenti *et al.* (2006) showed that there is an important effect of the coronal energy transport on event distribution. They studied statistical properties of solar coronal loops, subject to turbulent heating, to test whether the plasma response simply transmits the statistical distribution of events, with no modification. They found that for EUV lines the power-law index of the output distribution was strongly modified by becoming steeper (due to the dominance of radiative cooling), while for hotter lines ($T \approx 10^7$ K), where conductive cooling dominates the distribution is well preserved. This may explain the higher absolute values of α found for the very small events observed in EUV (cf. Figure 2) suggesting that for the Sun $\alpha \leqslant 2$.

On the other hand, similar flare statistics for solar-like stars give α values between -2.2 and -2.8 (Güdel 2007), suggesting that for stellar coronae flare heating is a viable option. Examples of stellar powerlaw distribution of a sample of 29 flares observed over a period of almost seven days on two solar-like stars 47 Cas and EK Dra are shown in

https://doi.org/10.1017/S1743921309030440 Published online by Cambridge University Press

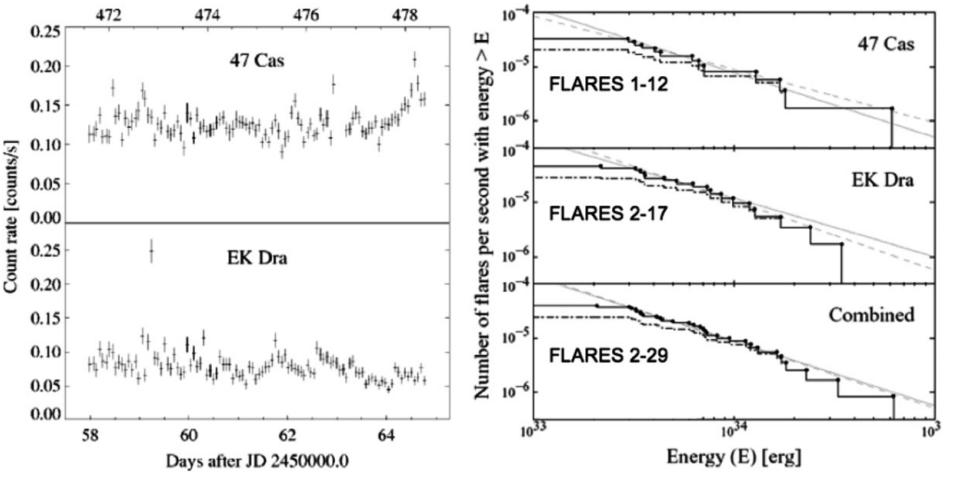

Figure 3. (*a*) Light-curves taken in the 40-190 Å range, using the *Extreme Ultraviolet Explorer* (EUVE) of two solar-like stars 47 Cas and EK Dra showing flaring. The bin-size corresponds to one EUVE orbit (96 min) (*b*) Powerlaws ($dN/dE \sim E^2$, with $\alpha \approx 2.2 \pm 0.2$) of stellar flare differential distribution *vs.* the total X-ray energy in the range between 3×10^{33} and 6×10^{34} ergs (adopted from Audard *et al.* 1999).

Figure 3, from Audard *et al.*(1999). Stellar flare observations are obviously sampling the highest-energy end of the flare distribution, less modified by transport effects.

2.5. *Standard model for eruptive solar flares*

The best-studied solar flares are the two-ribbon flares. Their unified model is often referred to as the CSHKP model (Carmichael 1964; Sturrock 1966; Hirayama 1974; Kopp & Pneuman 1976). However, the scenario has gone through important evolution since the publication of its main elements in the sixties and seventies (see *e.g.* Forbes 2001). A cartoon of the model and characteristic multi-wavelength light-curves are shown in Figure 4, while observations of a typical event is shown in Figure 5.

Two-ribbon flares occur in a dominantly bipolar magnetic configuration, with a filament along the magnetic inversion line (IL). As magnetic shear is increasing in the active region (with a concentration of shear in the vicinity of the IL) the filament is slowly rising (reaching a new equilibrium), stretching the enveloping bipolar magnetic arcade, leading to the formation of a current sheet under it (Figure 4b). There is, however, a point when new equilibrium is impossible and the filament starts accelerating and erupts. In the current sheet, which had formed under the erupting filament, magnetic reconnection takes place. Field lines break and change connectivity and magnetic field dissipates. The tension force of the reconnected field lines then accelerates the plasma out of the dissipation region. A subsequently in-flowing plasma carries the ambient magnetic field lines into the dissipation region. These field lines continue the reconnection cycle. Through this process, the magnetic energy stored near the current sheet or magnetic null-point is released to become the thermal and bulk-flow energy of the plasma. Magnetic energy is converted into heat and kinetic energy. Large electric fields are created in the dissipation region as well as shock waves, which help to accelerate particles. Since fast particles and heat conduction are mainly directed along the field lines, they will be channelled along the newly reconnected loops (Figure 4b). Electrons accelerated in the reconnection process gyrate along magnetic field lines emitting gyrosynchrotron radiation. Collisions in the dense chromosphere emit bremstrahlung observed in hard X-rays

https://doi.org/10.1017/S1743921309030440 Published online by Cambridge University Press

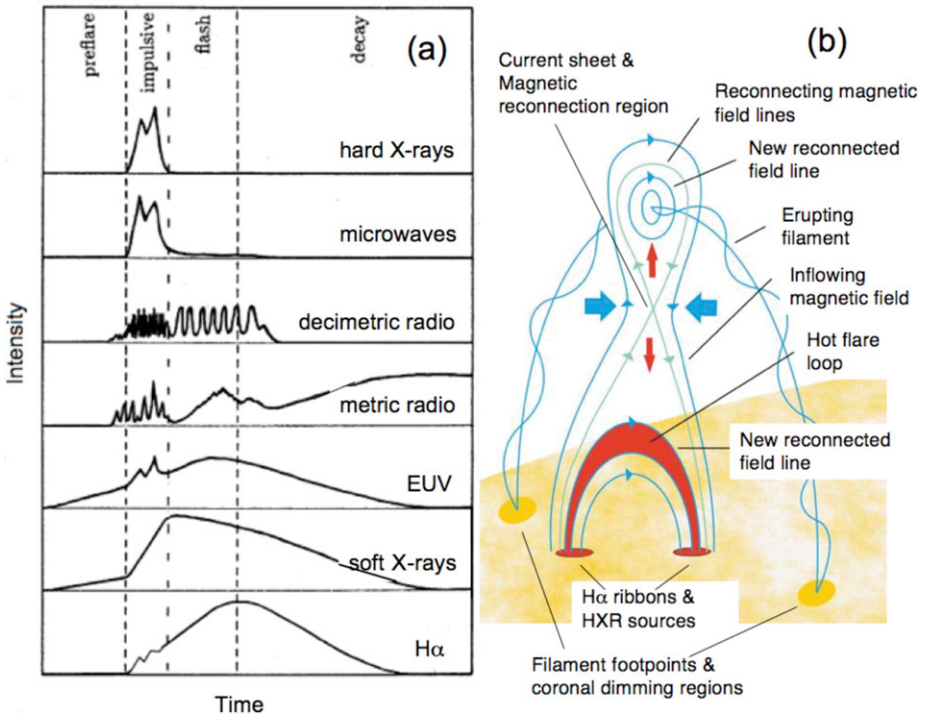

Figure 4. (*a*) Typical light-curves of a two-ribbon eruptive flare (LDE & CME) representing emissions from the chromosphere to the corona, adapted from Benz (2008). (*b*) Cartoon of a two-ribbon eruptive flare, adapted from Shibata (1998).

(HXRs; $\geqslant$ 20 keV). Accelerated electrons impulsively heat the chromosphere leading to optical and UV emission (e.g. flare ribbons seen in Hα). Heated chromospheric plasma expands upward, increasing the density and temperature in the reconnected coronal loops, leading to the formation of hot flare loops observed in EUV and SXRs. Continuing reconnection between field lines more and more distant from the IL leads to the formation of flare loops of increasing height while the flare ribbons at their footpoints are moving apart. Flares described by the CSHKP model are so-called long duration events (LDEs), which last for up to tens of hours (Figure 4a) and are invariably associated with coronal mass ejections (CMEs).

A few tenths of the total flare energy is released within a few minutes in the *impulsive phase* over a broad spectrum in HXRs, white light, UV, microwaves, etc. (Figure 4a). The radiations have an intermittent, bursty profile indicating patchy reconnection events along the long current sheet. During this phase important role is played by non-thermal electrons. In the decay phase reconnection is still taking place at increasing height along the lengthening current sheet at a gradually decreasing rate. The role of non-thermal particles is diminished, conduction fronts gaining importance instead.

In flares there is a very important relationship between HXRs and SXRs called the *Neupert effect* (Neupert, 1968). It expresses that SXRs mainly originate from plasma heated by the accumulated energy deposited by accelerated electrons from flare start(t_0).

$$F_{SXR}(t) \approx \int_{t_0}^{t} F_{HXR}(t)dt. \tag{2.1}$$

https://doi.org/10.1017/S1743921309030440 Published online by Cambridge University Press

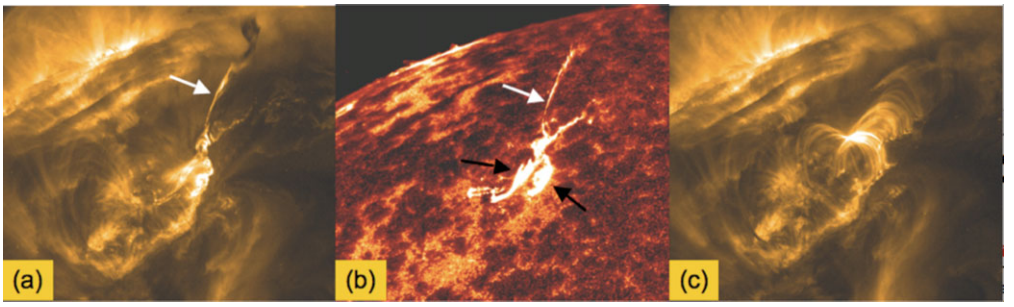

Figure 5. These TRACE spacecraft images were taken on 25 June 2000, (*a*) and (*b*) around 07:37UT and (*c*) 2h 10m later. The images were rotated, so that north is to the left. (*a*) White arrow points at a filament in the process of being ejected from the Sun, with cool (dark) and hot (bright; $\approx 1.5\,10^6$ degrees) material at opposite ends of the long, nearly vertical structure. (*b*) A 1600 Å image represents plasma of about 10^5 degrees, where the heated-up filament material (white arrow). The brightest features are flare ribbons (black arrows). (*c*) This 195 Å image shows a rapidly cooling arcade of flare loops in the late phase of the flare, when the flare ribbons at the footpoints of the flare loops have decreased in brightness.

The expression can be reversed, i.e. the derivative of SXR radiation shows similar time profile of that of the HXR or microwave radiation.

There are hundreds of papers providing evidence for the flare model described above. Here I can only mention a few which I consider to be the most important.

Using SOHO/EIT and Yohkoh/SXT data, an exceptionally clear evidence for the existence of the reconnection inflow was discovered by Yokoyama *et al.* (2001). They observed an eruptive flare on the solar limb, which displayed a geometry and scenario (e.g. filament eruption, cusp, X-point) highly resembling to the 2D reconnection cartoon shown in Figure 4(b). Following the filament eruption, a clear plasma motion with v = 1.0-4.7 km s^{-1} was observed towards the reconnection region (X-point). The reconnection rate, which is defined as the ratio of the inflow speed to the estimated Alfvén speed, derived from this observation was M_A = 0.001-0.03, which is roughly consistent with Petchek's (1964) fast reconnection model.

Observations of outflow from the reconnection region provide another key evidence. Forbes and Acton (1996) showed how newly formed cusped flare loops shrink and relax into a roughly semi-circular shape due to magnetic tension. McKenzie and Hudson (1999) discovered supra-arcade down-flows in LDEs at speeds between 40 and 500 km s^{-1}, confirming the existence of such outflow, indicating a patchy and intermittent reconnection process. Asai *et al.* (2004) showed that the start of these downflows are associated with HXR emission and microwave bursts observed with RHESSI and the Nobeyama radioheliograph, respectively. In radio wavelengths double type III bursts (due to electron beams propagating with $v \approx 0.2 - 0.6c$) are frequently observed propagating upward and downward from a common source at $\approx 0.9 - 5 \times 10^5$ km height in the corona (Benz, 2008 and references therein).

Multi-wavelength observations of flare ribbons also support the picture arising from the CSHKP model. RHESSI observations provided evidence that in flares HXR and γ-ray footpoint sources are co-spacial with the bright Hα and UV flare ribbons (Benz 2008 and references therein) and co-spatial with the highest magnetic flux densities and highest magnetic reconnection rates along the ribbons (Asai *et al.* 2002). Czaykowska *et al.* (1999) and Harra *et al.* (2005) using SOHO/CDS EUV spectroheliograms found bright down-flowing plasma to coincide with the ends of flare loops. The dimmer plasma on the outer side of the ribbons showed strong blue-shifts (upflows). Since the outer edge

https://doi.org/10.1017/S1743921309030440 Published online by Cambridge University Press

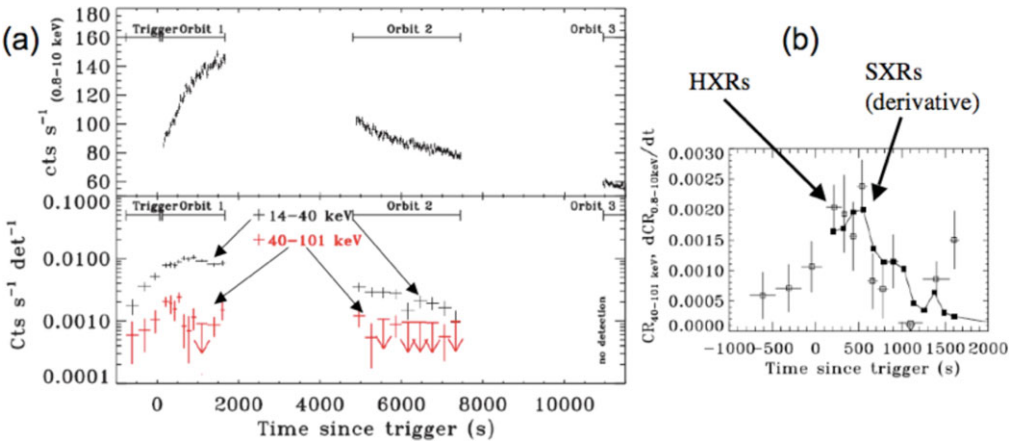

Figure 6. Swift observations of a stellar flare from II Peg on 16 December 2005 from the trigger at 11:21:52 UT from Osten *et al.* (2007). (*a*) Light curves from XRT, 0.8-10 keV (top) and two HXR energy bands from the BAT (14-40 and 40-101 keV; bottom). (*b*) Plot of 40-101 keV BAT light curve (open squares with error bars), along with scaled derivative of the XRT light curve for the first 2500 s of the flare. The correlation for roughly 1000 s after the trigger is consistent with the *Neupert effect*.

of flare ribbons are mapping to more recently reconnected loops than the inner edge, evaporation (blueshift) was observed at the outer edges, while downflows in the cooling loops mapped along the inner edge of flare ribbons.

LDEs are invariably associated with coronal mass ejections, of which the erupting flux rope containing the filament forms the core. Coronal mass ejections carry away typically 10^{15} g of solar material embedded in $10^{20} - 10^{22}$ Mx magnetic flux. Due to fast-decreasing pressure with height in the solar corona, CMEs expand. As suggested by Attrill *et al.* (2007), their magnetic fields meet with non-parallel fields of surrounding magnetic structures, current sheets form and dynamic reconnections take place. As a consequence, a large part of the Sun become CME constituent, supplying mass to the CME (van Driel-Gesztelyi *et al.* 2008 and references therein). Similar reconnection mechanism may lead to small flares in the wake of big stellar flares (Kővári *et al.* 2007).

2.6. *Solar-paradigm stellar flare*

Though stellar flares can release energy six orders of magnitude higher than that of a large solar flare, the energy release mechanism may not be very different of their solar equivalents. Osten *et al.* (2007) reported Swift observations of a large flare from the II Pegasi active binary system, which released a total energy of 10^{38} ergs (Figure 6). The SXR lightcurve of the flare (0.8-10 keV) closely resembles that of a solar LDE shown in Figure 4(a). The temperature of $\approx$80 MK was several factors higher than that of a big solar flare. The novelty of this observation is that the non-thermal component of a stellar flare was observed for the first time with Swift's high-energy channels (14-40 keV and 40-101 keV). The derivative of the SXR emission has a similar time-profile as the HXR emission, suggestive of the Neupert effect found for solar flares, implying that (coronal) SXRs mainly originate from plasma heated by accelerated particles impacting in denser (chromospheric) layers. For comparison, if II Pegasi was at a distance of 1 AU, the GOES classification of this flare would have been X4.4 $\times$ 10^6, while the largest solar flare ever observed was about X30 (the exact number was impossible to determine due to saturation of the detector)!

https://doi.org/10.1017/S1743921309030440 Published online by Cambridge University Press

3. Conclusions

Though all our observational proofs are indirect, reconnection seems to be at work at all scales in the solar atmosphere, releasing magnetic free energy mainly brought up by twisted flux emergence from the solar interior. To further understand details of the energy release process, we need high-resolution (vector) magnetic field measurements not only in the non-force-free photosphere, but in the chromosphere and the corona. Though simple 2D models are good starting points, we have to keep in mind that the events are in 3D. In order to understand observations we have to focus more on 3D modeling, embracing more complicated 3D reconnection models, e.g. the QSL concept.

For understanding stellar flares the solar paradigm is powerful, but it cannot cover all the physical conditions on active stars. On the Sun, flaring probability and importance increase with total magnetic flux, electric current and magnetic shear in the active region (e.g. Leka and Barnes, 2007) and with the flux in the vicinity of its high-gradient IL (Schrijver, 2007). On active stars, where large magnetic filling factors have been found (up to ≈80%; Berdyugina, 2005), active region flux may be two orders of magnitude higher than their solar counterparts. We have no information, however, on the non-potentiality of stellar magnetic fields and probably we underestimate their complexity. Flare energies exceed that of the solar flares by five-six orders of magnitude, therefore stellar flares in spite of sharing at least some of the essential physics with solar flares, cannot be regarded as their simple scaled-up versions. What makes the difference? The answer may differ for different stars.

Acknowledgements

The author thanks the TRACE Team for the data and acknowledges Hungarian government grant OTKA T048961.

References

Asai, A., Masuda, S., Yokoyama, T., Shimojo, M., Isobe, H., *et al.* 2002, *ApJ* 578, L91
Asai, A., Yokoyama, T., Shimojo, M., & Shibata, K. 2004, *ApJ* 605, L77
Aschwanden, M. J., Tarbell, T. D., Nightingale, R. W., *et al.* 2000, *ApJ* 535, 1047
Attrill, G. D. R., Harra, L. K., van Driel-Gesztelyi, L., & Démoulin, P. 2007, *ApJ* 656, L101
Audard, M., Güdel, M., & Guinan, E. F. 1999, *ApJ* 513, L53
Aulanier, G., Pariat, E., Démoulin, P., & DeVore, C. R. 2006, *Solar Phys.* 238, 347
Aulanier, G., Golub, L., DeLuca, E. E., Cirtain, J. W., Kano, R., *et al.* 2007, *Science* 318, 1588
Benz, A. O. 2008, *Living Rev. Solar Phys.* 5, 1
Berdyugina, S. V. 2005, *Living Rev. Solar Phys.* 2, 8
Carmichael, H. 1964, in W. N. Hess (ed.): *Physics of Solar flares*, NASA SP-50, 451
Czaykowska, A., De Pontieu, B., Alexander, D., & Rank, G. 1999, *ApJ* 521, L. 75.
Démoulin, P. 2007a, *Adv. Space Res.* 39, 1674
Démoulin, P. 2007b, *Adv. Space Res.* 39, 1367
Démoulin, P. & Berger, M. A. 2003, *Solar Phys.* 215, 203
Démoulin, P. & Pariat, E. 2008, *Adv. Space Res.*, submitted.
Démoulin, P., Priest, E. R., & Lonie, D. P. 1996, *JGR* 101, A4, 7631
Fan, Y. 2008, *ApJ* 676, 680
Forbes, T. G. 2000, *JGR* 105, A10, 23153
Forbes, T. G. & Acton, L. W. 1996, *ApJ* 459, 330
Güdel, M. 2007, *Living Rev. Solar Phys.* 4, 3
Harra, L. K., Démoulin, P., Mandrini, C. H., Matthews, S. A., van Driel-Gesztelyi, L., Culhane, J. L., & Fletcher, L. 2005, *A&A* 438, 1099
Hirayama, T. 1974, *Solar Phys.* 34, 323
Hudson, H. S. 1991, *Solar Phys.* 133, 357
Kopp, R. A. & Pneuman, G. W. 1976, *Solar Phys.* 50, 85

Kővári, Zs., Vilardell, F., Ribas, I., Vida, K., van Driel-Gesztelyi, L., Jordi, C., & Oláh, K. 2007, *AN* 328, 904
Leka, K. D. & Barnes, G. 2007, *ApJ* 656, 1173
Leka, K. D., Canfield, R. C., McClymont, A. N., & van Driel-Gesztelyi, L. 1996, *ApJ* 462, 547
Longcope, D. W., Linton, M. G., Pevtsov, A. A., Fisher, G. H., & Klapper, I. 1999, in M. R. Brown, R. C. Canfield, A. A. Pevtsov (eds.): *Magnetic helicity in Space and Laboratory Plasmas*, (Geophys. Monograph. 111, Washington D.C.: AGU), 93
López-Fuentes, M., Démoulin, P., Mandrini, C.H., & van Driel-Gesztelyi, L. 2000, *ApJ* 544, 540
Magara, T. 2004, *ApJ* 605, 480
Manchester, W., IV 2007, *ApJ* 666, 532
Manchester, W., IV, Gombosi, T., DeZeeuw, D., & Fan, Y. 2004, *ApJ* 610, 588
McKenzie, D. E. & Hudson, H. S. 1999, *ApJ* 519, 93
Meunier, N. 2005, *A&A* 443, 309.
Moreno-Insertis, F. & Emonet, T. *ApJ* 472, L53
Osten, R. A., Drake, S., Tueller, J., Cummings, J., Perri, M., Moretti, A., & Covino, S. 2007, *ApJ* 654, 1052
Pariat, E., Aulanier, G., Schmieder, B., *et al.* 2004, *ApJ* 614, 1099
Petchek, H. E. 1964, in *Physics of Solar flares*, ed. W. N. Hess, NASA SP-50, 425
Priest, E. R. & Forbes, T. 2000, *Magnetic Reconnection* Cambridge, UK: Cambridge University Press
Schrijver, C. J. 2007, *ApJ* 655, L117
Schrijver, C. J., DeRosa, M. L., Metcalf, T., Barnes, G., Lites, B. *et al.* 2008, *ApJ* 675, 1637
Schüssler, M. 1979, *A&A* 71, 79
Shibata, K. 1998, *Astrophys. Space Sci.* 264, 129
Sobotka, M., Vázquez, M., Bonet, J. A., Hanslmeier, A., & Hirzberger, J. 1999, *ApJ* 511, 436
Sturrock, P. A. 1966, *Nature* 211, 695
Švanda, M., Kosovichev, A. G., & Zhao, J. 2008, *ApJ* 680, L161
van Driel-Gesztelyi, L., Attrill, G. D. R., Démoulin, P., Mandrini, C. H., & Harra, L. K. 2008, *Ann. Geophys.* 26, 3077
Yokoyama, T., Akita, K., Morimoto, T., Inoue, K., & Newmark, J. 2001, *ApJ* 546, L69
Zhao, J. & Kosovichev, A. G. 2004, *ApJ* 603, 776.

Discussion

STRASSMEIER: You mentioned that no magnetic reconnection has ever be seen and that all evidence is indirect. Is this also the case for the most recent TRACE 171 Å movies?

VAN DRIEL-GESZTELYI: Only *consequences* of magnetic reconnection or changes due to reconnection are seen even in the highest-resolution observations. The reconnection region is small and it has low emission measure being difficult to observe. However, long current sheets where reconnection can happen have been observed in SOHO/UVCS and more recently in *Hinode*/XRT data.

ZINNECKER: My question focuses on young solar-mass stars before the Main Sequence, the T Tauri stars. We know that they have much larger X-ray luminosity than Main Sequence stars, due to gigantic loops filled with plasma. They also have enhanced flare activity. Now, what is the reason for such increased stellar activity, what is different in their magnetic field structure?

VAN DRIEL-GESZTELYI: Though the majority of models assume a simple bipolar field for the accreting T Tauri stars, in reality the field topology may well be much more complex. Complexity combined with high magnetic flux density would create long high-flux, high-gradient magnetic inversion lines, which have been shown to scale with flare activity on the Sun.